MODELING NORTHERN MID-LATITUDE GLACIATION WITH GCM-DRIVEN CLIMATE: FOCUS ON DEUTERONILUS-PROTONILUS MENSAE VALLEYS. J. L. Fastook[1], J. W. Head[2], J.-B. Madeleine[3], F. Forget[3], and D. R. Marchant[4] [1]University of Maine, Orono, ME 04469, fastook@maine.edu, [2]Brown University, Providence, RI 02912 . [3]LMD, CNRS/UPMC/IPSL, Paris, France. [4]Boston University, Boston MA.

Introduction: Investigations with models of paleo-ice sheets on Mars help identify and interpret glacial deposits observed from orbit [1, 2, 3] as well as aid in explaining the mechanisms that may have been responsible for the formation of the ice-rich mantling seen north of ~50°N latitude by GRS on Mars Odyssey [4]

The interesting story of how Mars at high obliquity (~45°) transfers water from current polar ice caps to the flanks of the large tropical volcanoes [2] continues, except now at lower obliquity (~35°) with water sources not at the poles, but instead on the tropical volcanoes.

Global Circulation Model Results: Work with a GCM [5] has produced a map of potential accumulation rates for the Dichotomy Boundary region, which can be used in an ice sheet model to describe a possible ice sheet with associated valley glaciation observed in the glacial geology [6, 7]. Figure 1(a) shows the distribution of positive net mass balance regions for one of 24 GCM runs from [5], corresponding to an obliquity of 35°, a dust opacity of 2.5, an eccentricity of 0.1, solar longitude of perihelion at 270°, and a water source in the Tharsis Region. With peak values of ice accumulation reaching 10 mm/a this pattern of mass balance is clearly capable of producing an ice sheet along the Dichotomy Boundary commensurate with the geological observations. As pointed out in [5], the broad region of positive mass balance north of 50° could explain the observed ice mantling [4].

Modeling: The University of Maine Ice Sheet Model (UMISM), as used here, is an adaptation for the Martian environment [8,9,10] of a thermo-mechanically coupled shallow-ice approximation terrestrial ice sheet model used for time-dependent reconstructions of Antarctic, Greenland, and paleo-ice sheet evolution in response to changing climate on Earth [11].

Clearly such a wide area of positive mass balance will create a broad, extensive ice sheet, as opposed to the localized valley glaciers observed in the geological record. For this reason we chose to focus attention on the Deuteronilus-Protonilus Mensae valley (DPM) described in [6]. Running the ice sheet model at a resolution sufficient to resolve the valley is prohibitive for such a broad area. We instead utilize the embedded-grid feature of UMISM.

This feature allows us to run a broad-domain, low-resolution grid with a more limited-domain, higher-resolution grid embedded within it. This embedded

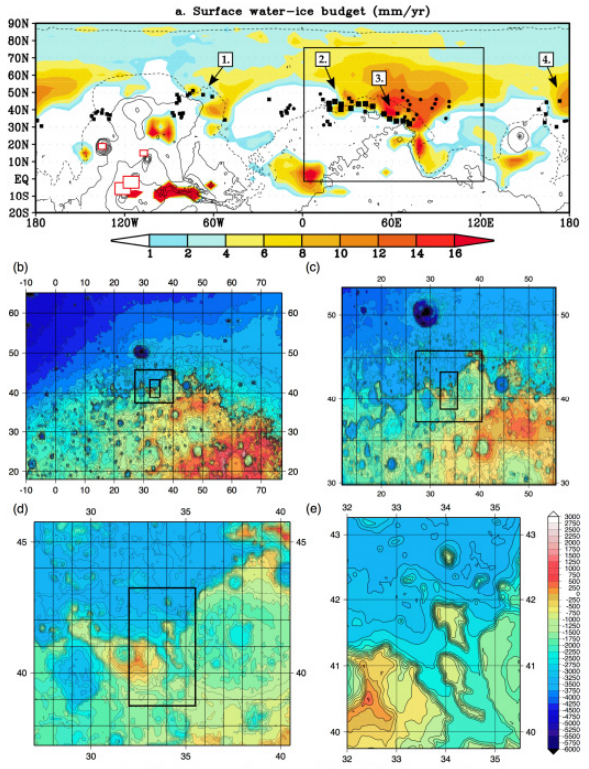

Figure 1: (a) GCM results from [5] and (b-e) nested grids.

grid obtains boundary condition information from a spatial and temporal interpolation of the low-resolution grid. Note that without this feature the limited-domain grid would require extensive manual specification along its boundary of either the flux or the ice thickness, both of which we would expect to change with time as the broad-scale ice sheet grew and shrank. This embedded feature allows us to nest grids, so that the jump in resolution is not so extreme as to produce spurious results.

The grids in the nest used in this exercise, with topography from MOLA, are also shown in Figure 1. Going from the broad grid (b) outlined in (a) with 10164 nodes and a resolution of 50 km the nest progresses to 16625 nodes and 12 km resolution (c), on to 7521 nodes and 6 km resolution (d), and finally to the highest resolution, 1.6 km with 12769 nodes (e).

With the relatively high accumulation rates predicted by [5], growth of a significant ice sheet is relatively rapid, and we permit growth under steady climate conditions for 600 Ka. At this point, we remove the positive accumulation component of the mass balance, leaving only the negative sublimation. This might be expected to occur if the source region in

Tharsis becomes depleted, or the obliquity changes, which is to be expected on approximately this time scale.

Figure 2 shows the surface, thickness, and velocity (rows 1, 2, and 3, label 4006) at 600 Ka in the DPM valley region. From the surface we see that the valley topography is almost completely drowned by the regional ice sheet, with ice approximately 3 km thick over the plateau, more than 4 km thick over the valley trunks, and as thin as 1.4 km over the aretes. Velocity, shown here logarithmically, is maximum over the valleys, typically a few 100 mm/a, dropping to less than 100 as it moves out onto the plains, and 1 to 10 mm/a over the plateau.

As the ice sheet sublimes, the surface drops and begins to reflect more clearly the underlying topography. At 800 Ka (col. 2, label 4102) the arêtes begin emerging as nunataks. Velocities are now considerably reduced to 1 mm/a in the valleys, and 0.001 mm/a on the plateaus. As collapse continues, the plateaus emerge (1100 Ka, col. 3, label 4105) and are fully cleared by 1200 Ka (col. 4, label 4106). At this point the ice in the valleys is less than 500 m thick, while on the plains it is still over 1 km. Of particular interest is the configuration at 1400 Ka (col. 5, label 4108), at which point only limited patches a few hundred meters thick remain surrounding one of the aretes on the plain outside the mouth of the valley, a configuration similar to the patterns reported by [6].

References: [1] J. Head and D. Marchant (2003) *Geology* 31, 641-644. [2] F. Forget et al. (2006) *Science* 311, 368-371. [3] J. Fastook et al. (2008) *Icarus* 198, 305-317. [4] B. Levard et al. (2004) *Nature* 431, 1072. [5] J.-B. Madeleine et al. (2008) *Icarus* submitted. [6] J. Head et al. (2006) *Geophys. Res. Lett.* 33, L08S03. [7] J. Fastook et al. (2008) LPSC 39 #1109. [8] J. Fastook et al. (2004) LPSC 35 #1352. [9] J. Fastook et al. (2005) LPSC 36 #1212. [10] J. Fastook et al. (2006) LPSC 37, #1794. [11] J. Fastook (1993) *Computational Science and Engineering* 1, 55-67.

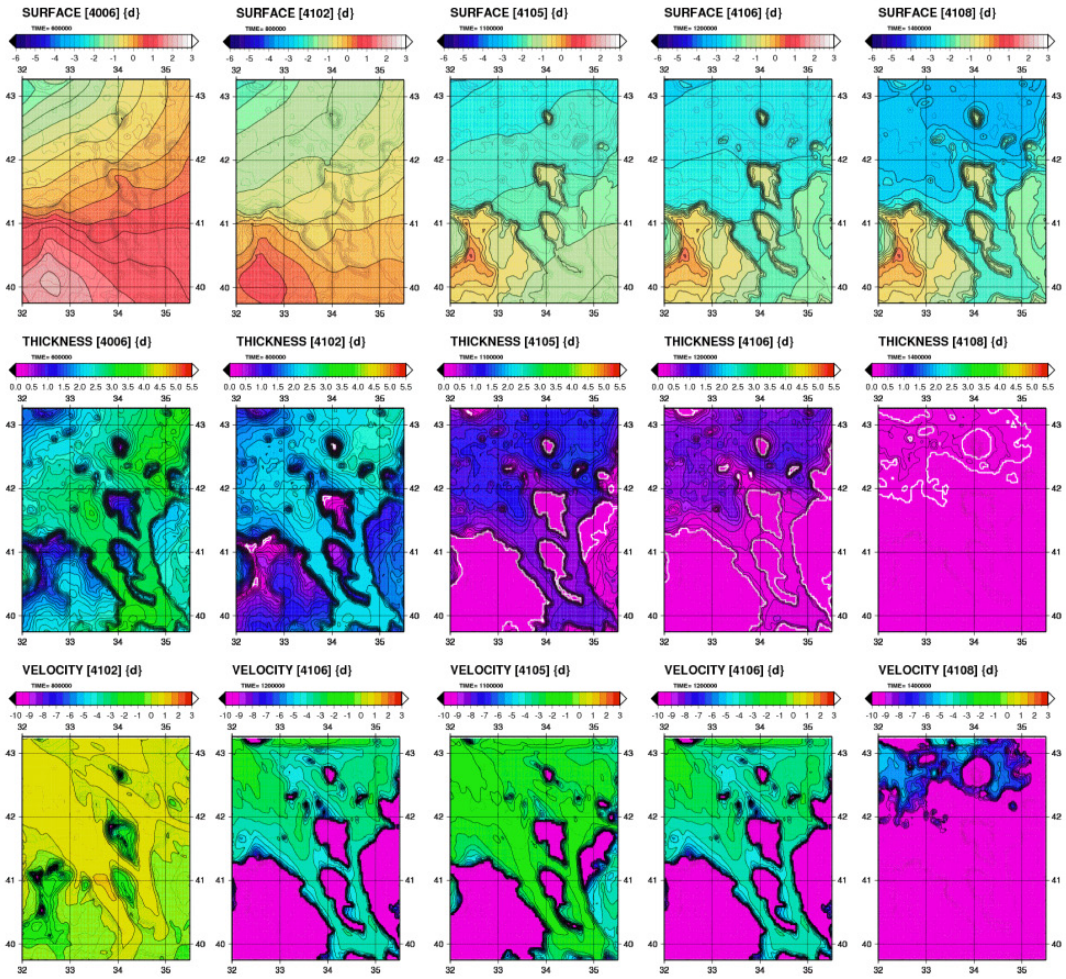

Figure 2: Surface, thickness, and velocity (rows 1-3) for times 600, 800,1100, 1200, and 1400 Ka (columns 1-5).